ELSEVIER

Applied Surface Science 182 (2001) 286–292

applied surface science

www.elsevier.com/locate/apsusc

Ion tracks — quasi one-dimensional nano-structures

G. Schiwietz[a,*], E. Luderer[a], P.L. Grande[b]

[a]*Hahn-Meitner-Institut, Strukturforschung SF4, Glienicker Street 100, 14109 Berlin, Germany*
[b]*Instituto de Física, Universidade Federal do, Rio Grande do Sul, 91500 Porto Alegre, Brazil*

Abstract

Our current understanding of the short-time interaction of fast heavy ions with matter is reviewed. Fast ions move along straight line trajectories and loose their energy mainly via collisions with electrons in the close surrounding of the ion path. Thus, the initial stages of corresponding ion tracks are highly excited cylindrical regions with diameters of the order of nanometers that extend over some micrometers in length. The energy dissipation inside these cylinders and the different possible pathways from dense electronic excitations to atomic motions and phase transitions are discussed in the light of recent experimental results.

PACS: 32.80.Hd; 31.70.Hq; 79.90.+b; 65.40.−b

Keywords: Ion tracks; Thermal spike; Coulomb explosion; Nano-structures

1. Introduction

Fast heavy ions may lead to permanent material changes in a small cylinder along the nearly straight ion path, giving rise to the so-called ion tracks. The appearance of track effects in polymers is known since some decades [1] and has found widespread applications in the meanwhile [2]. Nowadays, it is known that other insulators, semi-conductors and even metallic glasses [3,4] are also subject to materials modifications by heavy ions. Overlapping ion tracks (at high fluences) may, e.g. lead to enhanced interface mixing effects. Furthermore, macroscopic material changes, such as plastic deformation or surface instabilities, are induced by the electronic energy deposition inside ion tracks [3,4]. Individual ion tracks are explored as columnar defects for magnetic flux pinning [5] and as quasi one-dimensional wires for electron field emission [6]. They are also used to trigger and control the nucleation of metal clusters in glass, similar as in the photographic process [7].

Direct displacements due to the interaction between the fast projectile and individual target atoms (nuclear energy loss) can be excluded for the above mentioned effects. Only in a few cases, the modifications could be traced back to specific phase transitions [8]. Typically, track effects involve thresholds for the electronic energy transfers between the primary ion and the solid. Thus, they require a high electron energy density. The evolution from an electronically excited system to the permanent structural modification, however, is still under discussion.

There are a few models for the track-production mechanisms and until now, most of them cannot completely be ruled out. In order to point out, what are the weaknesses of our present knowledge, a short

* Corresponding author. Tel.: +49-30-8062-2448; fax: +49-30-8062-2293.
E-mail address: schiwietz@hmi.de (G. Schiwietz).

0169-4332/01/$ – see front matter
PII: S0169-4332(01)00415-9

review of the possible scenarios of the track evolution is given. Special emphasis is devoted to the short-time phenomena from the initial ion energy loss processes to the electronic de-excitation processes.

The first step of the nuclear-track evolution is the ionization and excitation of atoms close to ion path. The most important parameters that drive subsequent solid-state reactions are the local electron-energy density and the local ionization density, as will be explained below. Current experimental techniques do not have direct access to these quantities. The closely related total ion energy loss and the degree of inner-shell ionization, however, are subject to many investigations and they are discussed in Section 2 for the case of fast heavy ions.

After the initial energy-transfer by heavy ions, the center of the track is highly ionized. Depending on the ionization density and on the charge-neutralization time the mutual repulsion of target ions may convert a significant amount of electronic potential energy into atomic motion. This conversion mechanism is described by the Coulomb explosion model [9–11] and related models [12–14]. Coulomb explosion will be significant only if the charge-neutralization time exceeds 10^{-14} s for light target atoms. The corresponding electrostatic potential due to the positively charged target ions is discussed in Section 2. Theory, however, predicts neutralization times of about 10^{-16} s for free-electron gas-like metals, such as Al.

Thus, for many metals charge neutralization is too fast and Coulomb explosion cannot take place. In this case, however, electronic recombination might still be slow, leaving a hot electron gas at the center of the track. The thermal spike model [15–20] assumes that electronic excitation leads to the formation of a hot plasma and, via the electron–phonon coupling (equivalent to electron–atom collisions), to an increased thermal atomic motion. Thus, except for the efficiency of the electron–phonon coupling, the kinetic electron energy is the main ingredient in this model, as discussed in Section 3.

The relative importance of the mechanisms depends on the charge-neutralization time, on the strength of the modified inter-atomic forces and on the electron–phonon coupling constant. For highly excited ion tracks, all of these quantities are unknown and thus, the influence of a certain mechanism can only be determined experimentally. This, however, is complicated by the fact that atomic motion in solid matter may be converted into a stochastic motion on a time scale of 10^{-13} to 10^{-12} s, independent of the early stage of the evolution. One possible way to improve the interpretation of material modification effects is the investigation of prompt emitted 'particles' that carry information from the early evolution inside the track. Ejected electrons can be used as precursors of the corresponding transient material states. Electrons may be probes for the first 10^{-18} to 10^{-14} s of the track formation and energy dissipation. For reviews on transport of fast electrons and fast-ion-induced electron emission from solids, the reader is referred to [21–24].

In this work, we concentrate only on the solid-state interactions of fast ions (very fast compared to the Fermi velocity, or equivalently $\gg$25 keV/u) close to their equilibrium charge state. We will be concerned with projectiles at energies per mass unit of $E_p/M_p =$ 2 to 5 MeV/u, corresponding to about 10% the speed of light, where the nuclear energy loss is only a minor fraction of the total ion energy loss. Inside thin foils these ions serve as a nearly instantaneous source of excitation along their trajectory. They do neither change their charge state significantly, nor their energy or direction of motion. Thus, they excite and they probe the target without being significantly perturbed during the penetration.

2. Ion-energy loss, target ionization and neutralization

Low energy ions slow down due to a manyfold of different processes. These processes are the nuclear energy transfer, electron capture, excitation and ionization of both the target as well as the projectile. For few-electron systems, there exist accurate quantum-mechanical solutions of the time-dependent Schrödinger equation that account for the different energy-transfer mechanisms, yielding stopping powers that agree to within a few percent with the experimental data [25–27], even for differential energy-transfer probabilities [28]. The situation is less satisfying for many-electron systems as they are typical for ion-solid interactions. However, the whole treatment simplifies again if we restrict ourselves to fast projectiles.

Fast ions loose their kinetic energy mainly through ionization of atoms from all shells and to some extent through excitation of valence- and conduction-band states. These energy-loss mechanisms are expected to be qualitatively well understood. Different attempts for a precise description of the energy loss of swift heavy ions in multi-electron targets are currently being worked out [29–36]. These approaches yield reasonable agreement among themselves as well as with the experimental data, as far as projectile energies above 1 MeV/u are considered. Some of the models yields the initial energy deposition as function of the distance from the track, a quantity that directly enters the thermal spike model. Hence, nowadays there are energy-loss models available that are more accurate than most other ingredient of the track models.

The energy loss due to ionization may always be decomposed into a mean transferred energy and an ionization probability P_b. The ionization probability is one of the central parameters of the Coulomb explosion model. Using Auger electron or X-ray spectroscopy one may determine the degree of multiple ionization of inner shells from the fractional hypersatellite intensities. Hypersatellite lines result from multiple inner-shell vacancies that reduce the screening and increase the Auger transition energies. As an example, double K-shell ionization of carbon atoms in different matrices will be considered here.

Fig. 1 displays the ratio of double to single ionization events corresponding to the interaction of particles with different characteristic energy losses, from incident electrons to highly charged U ions in their equilibrium charge state. The data have been extracted from Auger line intensities, considering electron escape depths, Auger cascades, and δ-electron collision cascades [37,38]. Here we have averaged our results for amorphous carbon [39–41], diamond-like carbon (DLC)[1] [32] and crystalline graphite, since the K-shell double ionization ratio does not significantly depend on the structure of the carbon target. All recent measurements (with incident electrons and heavy ions at 2 and 5 MeV/u) have been performed with a new ultra-high vacuum setup ensuring low surface contaminations.

[1] Diamond-like carbon films on a Si substrate, produced by B. Schultrich et al. (Dresden).

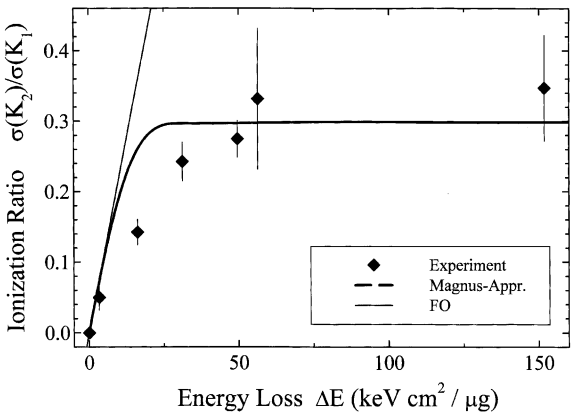

Fig. 1. Ratio of double to single ionization cross sections versus the specific projectile energy-loss (see text).

The theoretical curves are quantum results calculated for bare ions at 5 MeV/u. In an independent electron model (IEM) within first-order perturbation theory (FO) [42], one expects the ratio R to be roughly proportional to the electronic stopping power S_e. For the heavy ions Ni, Kr and U with high energy losses, however, there is a clear saturation in the data. The dashed curve in the figure is a theoretical result, calculated within the Magnus approximation [27] for numerical wavefunctions being eigenstates of a spherically averaged solid-state potential. It is still based on the IEM, but goes beyond perturbation theory. There is a qualitative agreement between these theoretical results and the data, the saturation values being the same.

The ionization probabilities in the Magnus approximation are close to 100% for heavy ions at small impact parameters. This leads to the saturation observed in Fig. 1. The overestimated double-ionization cross sections for small energy losses are due to the neglect of dynamic screening and electron correlation in the double ionization process. Taking this failure of our model results into account, we estimate that there is complete ionization of the K-shell as well as the valence band of carbon in central collisions with projectiles exceeding about 40 keV cm^2/μg.

Such a strong ionization of atoms close to the ion track leads to a positive potential, the nuclear-track potential [43,44], which is possible to detect if the charge neutralization is slow. This potential accelerates positive target ions and decelerates emitted

electrons. Line structures in the electron spectrum, i.e. the convoy electron peak due to electrons that move approximately with the projectile speed in the projectile direction or Auger lines, may be used to determine this deceleration. In fact, significant decelerations of Auger electrons corresponding to 1.1×10^{-14} s after the interaction [43,44] as well as of convoy electrons [45] due to microscopic potentials have been found for the insulators polypropylene (C_3H_6) as well as mylar. For Ne^{9+} ions at 5 MeV/u with only moderate energy losses, e.g. we have determined a track potential of 42 V [32,43,44], after correcting for some macroscopic charging of the samples. Thus, for heavy projectile ions the repulsive forces between the highly ionized atoms in the center of the track should exceed the binding forces by far. Consequently, atomic rearrangement and atom ejection (desorption) will appear for these materials with slow neutralization rates. In fact, giant chemical modification and desorption effects have been determined for polypropylene [32,43,44]. These results as well as the energy spectra of ejected ions from other hydrocarbon surfaces [46] point to the importance of the Coulomb explosion mechanism for some polymers.

For other carbon structures, such as diamond-like amorphous carbon (with sp^3 bonds) and graphite-like amorphous carbon as well as crystalline graphite (both with sp^2 bonds), Auger energy-shifts are below 2 eV. Thus, recombination is much faster in these materials and Coulomb explosion cannot be efficient. As an alternative to the Auger analysis, it is also possible to investigate track effects using the so-called convoy electrons. At an electron ejection angle of 0° with respect to the beam and for a velocity equal to the projectile speed a cusp-shaped peak appears in the spectrum of ejected electrons. This peak is due to capture and loss of electrons into low-lying continuum states of the projectile. Both processes have been investigated intensively for gas targets and a similar peak, named convoy-electron peak, was also found for solid-state targets.

Fig. 2 shows the energy distribution of 0°-electrons in the vicinity of the projectile velocity, for 5 MeV/u S^{13+} ions penetrating a thin graphite-like amorphous carbon-foil (a-C of about 70 atomic layers). The spectrum consists of three structures; the dominant and nearly symmetric convoy-electron peak [45], a broad shoulder on the high-energy side due to

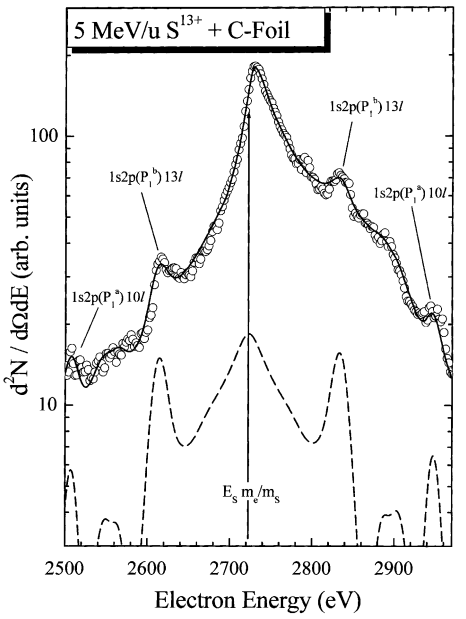

Fig. 2. Convoy-electron spectrum for 5 MeV/u S^{13+} ions penetrating evaporated (graphite-like) carbon with a thickness of about 3 μg/cm^2. The solid curve is a fit to the data, considering the different electron-production mechanisms. The dashed curve is estimated from the calculated autoioniozation energies and the spectrometer resolution. The arrow indicates the projectile velocity, as described in the text.

field-ionized Rydberg electrons [47,48] and a series of autoionization lines due to low-energetic doubly excited projectile states (for a review, see [49]).

These doubly excited states decay mainly behind the foil. Each of the lines appears twice in the spectrum, corresponding to forward and backward emission in the projectile frame. Thus, the center velocity of the lines, indicated by the vertical arrow, corresponds to the final projectile velocity. Comparison with the convoy peak maximum shows an acceleration of the convoy electrons by 5 ± 1.5 eV.

This acceleration is consistent with the negative image potential induced by the positively charged ion at the surface [45]. Thus, there is no significant deceleration due to a nuclear-track potential. Quantitative estimates indicate that the charge neutralization time is $<4 \times 10^{-16}$ s within tracks in a-C. This short-time interval is completely inconsistent with atomic motion driven by the Coulomb explosion mechanism. Now the question arises how electronic excitations

may be converted to atomic motions in the case of fast neutralization inside the track.

3. Electron temperatures and thermal spike

In this section, we will discuss the possibility of the thermal spike as a result of highly excited track cores after neutralization. The slope of the Auger lines carries information about the degree of excitation of the valence band during the Kr decay. The high energy shoulder of the Auger structures reflects a convolution of the populated density of states near the Fermi level [50,51]. As described in detail in previous publications [39–41] the line widths increase with increasing projectile charge-state, or with increasing electron temperature. The data evaluation is based on a comparison with Auger spectra for incident electrons, as a reference for the electron transport properties. Thus, we fit these electron induced spectra using a simple model for electron transport [52] that includes the density of states, assuming that the corresponding electron temperature in the valence band is nearly zero. Electron temperatures are than extracted from fits to ion induced spectra, by variation of the Fermi–Dirac distribution and by keeping all other transport properties fixed.

Fig. 3 displays electron temperatures T_e for two different Auger decay rates, corresponding to single (closed symbols for a decay time $\tau_{K_1} = 11 \times 10^{-15}$ s) and double (open symbols for $\tau_{K_2} = 6 \times 10^{-15}$ s)

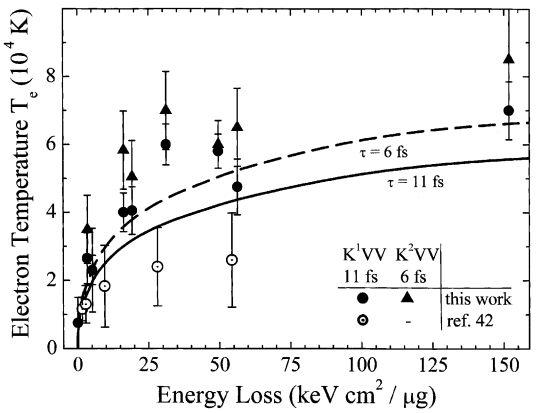

Fig. 3. Electron temperature as determined from the broadening of two Auger lines for three types of C and different projectile species in comparison with model calculations (see text).

K-vacancy states. Thus, together with the data in Fig. 1, we have three snapshots of the time evolution of electronic processes in highly excited tracks. Data for graphite-like amorphous carbon (a-C) [39–41], amorphous DLC, as well as for crystalline graphite (HOPG) have been averaged in this plot. The measured electron temperatures do not show significant deviations between these three materials.

A large fraction of the present results have been taken with a new ultra-high vacuum setup. The residual-gas was dominated by H_2 with total pressures between 10^{-10} and 10^{-9} mbar during the different beam times. The HOPG samples were cleaved and the DLC samples were heated to about 500 K prior to the final measurements. For both target types we have observed beam induced desorption, leading to negligible O surface coverages after some minutes of irradiation.

Note that we have included unpublished results for electron temperatures in a-C by Caron and Rothard in Fig. 3 [53,54]. These temperatures have been determined from Auger spectra induced by heavy ions at 9 MeV/u in a completely different way. A deconvolution technique was used to derive the density of states and no reference spectra for the zero-temperature case were utilized. Only single K-vacancy results are given because of limited counting statistics. These data agree well with our results for low energy losses. At higher energy losses an increasing deviation between both data sets is visible.

Theoretical curves calculated for decay times of 6 and 11 fs and ions at 5 MeV/u in a-C are shown for comparison [39–41]. This model includes the impact-parameter distribution of the initial energy deposition involving different types of Auger processes as well as transport of δ-electrons. The time dependence of the corresponding electron temperature is then calculated from the heat diffusion equation using ab initio values for the electronic transport properties.

The experimental as well as the theoretical data points show a slow increase of T_e as function of the electronic energy loss. For high projectile energy-losses electron temperatures of about 80,000 K are reached. On the average do our experimental results exceed the theoretical predictions by about 35% (the data by Caron and Rothard are up to a factor of 1.5 below the theoretical results). The relative energy dependence and the temperature ratio for

6 and 11 fs agree very well between theory and the present data. Thus, it seems as if these high electronic excitations in the center of the track are theoretically relatively well understood. The insensitivity with respect to the crystal structure, however, is not clear yet. An explanation might be the electron transport at high temperatures. High electron temperatures lead to a local modification of the electron–atom scattering potentials and furthermore, electron–electron scattering gains importance. Both effects might be similar for the three types of carbon and call for further investigation.

From the ratio $T_e(11\ \text{fs})/T_e(6\ \text{fs})$ one may estimate a track-relaxation time of about 25 ± 9 fs. In view of the high electron temperatures this might lead to lattice temperatures in excess of the melting point. Indication for the corresponding phase transitions have been found in macroscopic conductivity increases of a-C samples [39–41] as well as in conducting tracks with nanometer diameters within a DLC matrix [6].

4. Conclusions

The formation of quasi one-dimensional nanostructures (ion tracks) due to fast heavy ions is investigated with special attention on possible materials-modification mechanisms. The energy loss of fast ions is reasonably well understood for the explanation of track effects. The same holds true for the comparison of experimental and theoretical yields for multiple inner-shell ionization. For very heavy ions these results indicate that the center of the track is completely ionized, including the carbon K-shell electrons. Hence, the main unsolved question concerning material modifications by fast ions is "how are electronic excitations converted into atomic motion?". In this work, we have presented and discussed electron spectroscopy results for different modifications of carbon, i.e. crystalline graphite, graphite- and diamond-like amorphous carbon and polypropylene ($[C_3H_6]_n$).

For the latter material, we have found strong indications for the Coulomb explosion mechanism, a mutual repulsion of highly ionized atoms. For the other target materials, fast neutralization of the track and high electron temperatures have been found. Hence, Coulomb explosion can definitely be ruled out. The electron temperatures may lead to materials modifications via the electron–phonon coupling (thermal spike model) or via the modified inter-atomic forces resulting from the non-equilibrium electron densities. So far, it is not possible to distinguish between the latter two energy-conversion mechanisms on a pure experimental basis. From the present electron-spectroscopy work, however, it becomes clear that the pathways for materials modifications by fast heavy ions (Coulomb explosion versus thermal spike) are strongly dependent on the type of material.

Acknowledgements

This work was partially supported by the PROBRAL contract between DAAD and CAPES. We would like to thank K. Czerski for helpful comments on the present manuscript.

References

[1] R.L. Fleischer, P.B. Price, R.M. Walker, Nuclear Tracks in Solids, University of California Press, Berkely, CA, 1975.
[2] R. Spohr, Ion Tracks and Microtechnology, F. Vieweg und Sohn Verlagsgesellschaft, Braunschweig, 1990.
[3] S. Klaumünzer, M.D. Hou, G. Schumacher, Phys. Rev. Lett. 57 (1986) 850.
[4] A. Gutzmann, S. Klaumünzer, P. Meier, Phys. Rev. Lett. 74 (1995) 2256–2259.
[5] C. Müller, P. Mayewski, S. Klaumünzer, F. Aldinger, Nucl. Instr. Meth. B146 (1998) 555–580.
[6] M. Waiblinger, Ch. Sommerhalter, B. Pietzak, J. Krauser, B. Mertesacker, M.Ch. Lux-Steiner, A. Weidinger, C. Ronning, H. Hofsäs, Appl. Phys. A69 (1999) 239–240.
[7] E. Valentin, H. Bernas, C. Ricolleau, F. Creuzet, Phys. Rev. Lett. 86 (2001) 99.
[8] M. Boccanfuso, A. Benyagoub, M. Toulemonde, C. Trautmann, K. Schwartz, Ch. Dufur, Nucl. Instr. Meth. B 175–177 (2001) 590–593.
[9] R.E. Johnson, W.L. Brown, Nucl. Instr. Meth. B198 (1982) 103–118.
[10] A. Akkermann, J. Levinson, D. Ilberg, Y. Lifshitz, in: R. Baragiola (Ed.), Ionization of Solids by Heavy Particles, NATO Advanced Study Institutes Series 306, Plenum Press, New York, 1992, pp. 431–438.
[11] D. Leseur, A. Dunlop, Rad. Eff. Def. Solids 126 (1993) 163–172.
[12] C.C. Watson, T.A. Tombrello, Radiat. Eff. 89 (1985) 263–283.
[13] P. Stampfli, K.H. Bennemann, Phys. Rev. B49 (1994) 7299.
[14] P. Stampfli, Nucl. Instr. Meth. 107 (1996) 138.
[15] F. Desauer, Z. Phys. 12 (1923) 38.
[16] I.M. Lifshitz, M.I. Kaganov, L.V. Tanatarov, J. Nucl. Energy 12 (1960) 69.

[17] R.H. Ritchie, C. Claussen, Nucl. Instr. Meth. B198 (1982) 133–138.
[18] Z.G. Wang, C. Dufour, E. Paumier, M. Toulemonde, J. Phys. Condens. Matter 6 (1994) 6733.
[19] G. Szenes, Nucl. Instr. Meth. B116 (1996) 141.
[20] A.E. Volkov, V.A. Borodin, Nucl. Instr. Meth. 107 (1996) 172.
[21] R.D. Birkhoff, in: S. Flügge (Ed.), Handbuch der Physik, Vol. 34, Springer, Berlin, 1958, pp. 53–138.
[22] M. Rösler, W. Brauer, and also D. Hasselkamp, Particle Induced Electron Emission, Springer Tracts of Modern Physics, Vol. 123, Springer, Berlin, 1991.
[23] G. Schiwietz, in: R. Baragiola (Ed.), Ionization of Solids by Heavy Particles, NATO Advanced Study Institutes Series 306, Plenum Press, New York, 1992, pp. 197–214.
[24] H. Rothard, Swift heavy ion induced electron emission from solids, Scanning Microscopy 9 (1995) 1–42.
[25] G. Schiwietz, P.L. Grande, Nucl. Instr. Meth. B69 (1992) 10–17.
[26] P.L. Grande, G. Schiwietz, Phys. Rev. 47 (1993) 1119–1122.
[27] G. Schiwietz, P.L. Grande, Radiation effects and defects in solids 130/131 (1994) 137–156, and references therein.
[28] G. Schiwietz, P.L. Grande, C. Auth, H. Winter, A. Salin, Phys. Rev. Lett. 72 (1994) 2159–2162.
[29] P.L. Grande, G. Schiwietz, Phys. Rev. 58 (1998) 3796–3801.
[30] G. Schiwietz, P.L. Grande, Nucl. Instr. Meth. B153 (1999) 1–9.
[31] G.d.e.M. Azevedo, P.L. Grande, G. Schiwietz, Nucl. Instr. Meth. B164/165 (2000) 203.
[32] G. Schiwietz, E. Luderer, G. Xiao, P.L. Grande, Nucl. Instr. Meth. B 175–177 (2001) 1–11.
[33] The casp code for the UCA and PCA energy-loss theory may be downloaded from http://www.hmi.de/people/schiwietz/casp.html
[34] P. Sigmund, Nucl. Instr. Meth. B135 (1998) 1–15.
[35] A. Schinner, P. Sigmund, Nucl. Instr. Meth. B 174 (2001) 535–540.
[36] G. Maynard, M. Chabot, D. Gardes, Nucl. Instr. Meth. B164/165 (2000) 139–146.
[37] G. Schiwietz, D. Schneider, J.P. Biersack, N. Stolterfoht, D. Fink, A. Mattis, B. Skogvall, H. Altevogt, V. Montemayor, U. Stettner, Phys. Rev. Lett. 61 (1988) 2677.
[38] D. Schneider, G. Schiwietz, D. DeWitt, Phys. Rev. 47 (1992) 3945–3950.
[39] G. Schiwietz, G. Xiao, P.L. Grande, E. Luderer, R. Pazirandeh, U. Stettner, Nucl. Instr. Meth. B146 (1998) 131–136.
[40] G. Schiwietz, G. Xiao, P.L. Grande, E. Luderer, R. Pazirandeh, U. Stettner, Europhys. Lett. 47 (1999) 384–390.
[41] G. Schiwietz, G. Xiao, E. Luderer, P.L. Grande, Nucl. Instr. Meth. B164/165 (2000) 353–364.
[42] H.A. Bethe, R.W. Jackiw, Intermediate Quantum Mechanics, 2nd Edition, W.A. Benjamin Inc., 1968.
[43] G. Schiwietz, P.L. Grande, B. Skogvall, J.P. Biersack, R. Köhrbrück, K. Sommer, A. Schmoldt, P. Goppelt, I. Kádár, S. Ricz, U. Stettner, Phys. Rev. Lett. 69 (1992) 628.
[44] G. Schiwietz, G. Xiao, Nucl. Instr. Meth. 107 (1996) 113.
[45] G. Xiao, G. Schiwietz, P.L. Grande, A. Schmoldt, N. Stolterfoht, M. Grether, R. Köhrbrück, A. Spieler, U. Stettner, Phys. Rev. Lett. 79 (1997) 1821.
[46] K. Wien, Ch. Koch, N. van Tan, Nucl. Instr. Meth. B100 (1995) 322.
[47] D. Schneider, W. Zeitz, R. Kowallik, G. Schiwietz, T. Schneider, N. Stolterfoht, U. Wille, Phys. Rev. A34 (1986) 169.
[48] G. Schiwietz, D. Schneider, J. Tanis, Phys. Rev. Lett. 9 (1987) 1561.
[49] N. Stolterfoht, Phys. Rep. 146 (1987) 315.
[50] G. Galli, R.M. Martin, R. Car, M. Parrinello, Phys. Rev. B42 (1990) 7470.
[51] J. Schäfer, J. Ristein, R. Graupner, L. Ley, U. Stephan, Th. Frauenheim, V.S. Veerasamy, G.A.J. Amaratunga, M. Weiler, H. Erhardt, Phys. Rev. 53 (1996) 7762.
[52] S. Tougaard, P. Sigmund, Phys. Rev. B25 (1982) 4452–4466.
[53] M. Caron, H. Rothard, M. Beuve, B. Gervais (submitted for publication).
[54] M. Caron, PhD thesis, Caen, 2000.